

# On the Criteria of Instability for Electrochemical Systems

LI, Ze-Lin<sup>\*,a,c</sup>(李则林) REN, Bin<sup>b</sup>(任斌) NIU, Zhen-Jiang<sup>a</sup>(牛振江)

XIAO, Xiao-Ming<sup>c</sup>(肖小明) ZENG, Yue<sup>c</sup>(曾跃) TIAN, Zhong-Qun<sup>b</sup>(田中群)

<sup>a</sup> Institute of Physical Chemistry, Zhejiang Normal University, Jinhua, Zhejiang 321004, China

<sup>b</sup> State Key Laboratory for Physical Chemistry of Solid Surfaces and Department of Chemistry, Xiamen University, Xiamen, Fujian 361005, China

<sup>c</sup> Department of Chemistry, Hunan Normal University, Changsha, Hunan 410081, China

Both cyclic-voltammetry-based and impedance-based experimental criteria that have been developed recently for the oscillatory electrochemical systems are critically appraised with two typical categories of oscillators. Consistent conclusions can be drawn by the two criteria for the category of oscillators that involve the coupling of charge transfer mainly with surface steps (*e. g.* ad- and desorption) such as in the electrooxidation of C<sub>1</sub> organic molecules. Whereas, impedance-based criterion is not applicable to the category of oscillators that involve the coupling of charge transfer mainly with mass transfer (*e. g.* diffusion and convection) such as in the Fe(CN)<sub>6</sub><sup>3-</sup> reduction accompanying periodic hydrogen evolution. The reason is that the negative impedance cannot include the feedback information of convection mass transfer induced by the hydrogen evolution. However, both positive and negative nonlinear feedbacks, *i. e.*, the diffusion-limited depletion and convection-enhanced replenishment of the Fe(CN)<sub>6</sub><sup>3-</sup> surface concentration, that coexist between the bistability, *i. e.*, Fe(CN)<sub>6</sub><sup>3-</sup> reduction with and without hydrogen evolution at lower and higher potential sides respectively, are all reflected in the crossed cyclic voltammogram (CCV). It can be concluded that the voltammetry-based criterion (in time domain) is more intuitive, less time-consuming and has a wider range of applications than the impedance-based one (in frequency domain).

**Keywords** electrochemical oscillations, criteria for instability, cyclic voltammograms, impedance spectroscopy, C<sub>1</sub> organic molecules, ferricyanide

## Experimental criteria for electrochemical oscillatory systems

Since the first publication<sup>1,2</sup> by Fechner in 1828, oscillatory phenomena have been reported for a number of electrochemical processes, including electrodeposition and electrodisolution of metals, polarographic reduction, electrocatalytic oxidation of small organic molecules, and so on.<sup>2-4</sup> Recently, systematically mechanistic classifications of electrochemical oscillators and prediction for instability of electrochemical systems have been developed. For example, the impedance spectrum over a broad enough frequency range represents the linear information of the system correlative to the bifurcation analysis of instability.<sup>5</sup> On the basis of impedance spectroscopy, Koper classified electrochemical oscillators mainly into two categories. One category exhibits negative real impedance, including the zero frequency (Fig. 1a) which corresponds to a negative slope in the steady-state current-voltage curve. Current oscillations only occur exactly around the descending branch in the current-voltage curve. The other category has "hidden" negative impedance. In this case the frequency-dependent real impedance has a negative part for a range of non-zero frequencies, but becomes positive at zero frequency (Fig. 1b), corresponding to a positive slope in the steady-state current-voltage curve.

\* E-mail: wujina@sparc2.hunnu.edu.cn

Received June 11, 2001; revised February 7, 2002; accepted March 25, 2002.

Project supported by the National Natural Science Foundation of China (Nos. 20073012, 29833060, 29903009), and the Visiting Scholar Foundation (No. [1999] 153) in State Key Labs of Education Ministry of China.

Oscillations appear around this positive-sloped branch in the current-voltage curve under galvanostatic control, as well as under potentiostatic control in the presence of a sufficiently large ohmic drop.

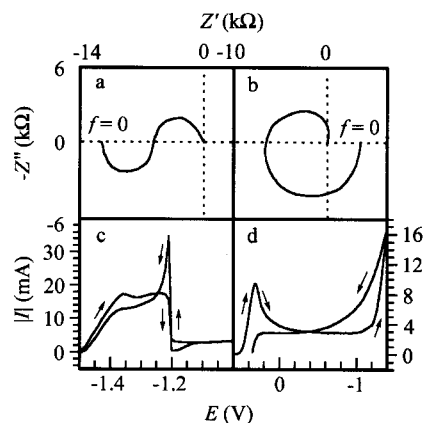


**Fig. 1** Typical profiles of Nyquist diagrams and cyclic voltammograms for electrochemical oscillatory systems with (a) and (c) current oscillations only, and with (b) and (d) both current and potential oscillations. (a) 9 mmol/L  $\text{In}^{3+}$  reduction on a HMDE in 5 mol/L NaSCN solution, (b) 0.1 mol/L HCHO in 0.1 mol/L NaOH on a rhodium RDE, (c) electrodisolution of a Zn disk with a 3 mm diameter in 5 mol/L NaOH, (d) 0.8 mol/L  $\text{Fe}(\text{CN})_6^{3-}$  reduction in 1 mol/L NaOH on a 3 mm diameter Pt disk. Figs. (a)—(b) and (c)—(d) are adapted from refs. 5 and 6, respectively.

Another universal criterion<sup>6</sup> with respect to oscillatory electrochemical systems is based on the cyclic voltammetry, which provides with a simplest intuition prediction for the instability of electrochemical systems. A cross occurs in the cyclic voltammograms from the forward and backward potential scan (Figs. 1c and 1d), and the closed loop that forms by the crossed curves is called a crossing cycle, of which the current value of the backward scan is larger than that of the forward scan. The crossing cycle apparently results from two opposite kinetic processes. One decreases the current value such as by passivation as in the Zn electrodisolution (Fig. 1c), and by depletion of reactant surface concentration under diffusion control as in the  $\text{Fe}(\text{CN})_6^{3-}$  reduction (Fig. 1d). The other increases the current such as by active dissolution (Fig. 1c) or by enhanced convection mass transfer through hydrogen evolution (Fig. 1d). Therefore, the crossing cycle manifests that there are a pair of overlapping positive and negative nonlinear feedbacks between

the bistable states (active-passive and with-without hydrogen evolution in Figs. 1c and 1d, respectively). It is a typical topology for electrochemical oscillatory systems.<sup>6</sup> The word “overlapping” means here that the positive and negative feedbacks coexist in a range of potentials, and predominate alternatively during the oscillation. Figs. 1c and 1d are typical cyclic voltammograms for systems that show current oscillations only<sup>6</sup> and that display both current and potential oscillations,<sup>7-8</sup> respectively. Note that the descending branch (forward potential scan) and the ascending branch (backward potential scan) in Fig. 1c are steep and close to each other, *i. e.*, the potential interval for the negative and positive feedbacks is too narrow to allow potential oscillations to occur with observable amplitudes. The size of the crossing cycle depends on the scan rate for a given oscillatory system. Experimentally, a scan rate of 100 mV/s is fast enough and is chosen for all of our previous and present work. At this scan rate, the size of the crossing cycle can be adjusted by other experimental parameters such as concentration, pH, temperature and so on, in order to match the positive and negative feedback strength properly for oscillation. A larger crossing cycle implies a much stronger negative feedback that drives the system to its initial state, and is generally favorable to generate oscillation. It is a useful way to realize oscillation with the help of the crossing cycle.

The remarkable advantage of the above two experimental criteria is that prediction for instability can be made without knowledge about the exact oscillatory mechanism, as well as the mathematical model. However, no work has been made up to date in the study of the relationship and the difference between the two criteria. In this article, the criteria are compared and examined by two typical categories of electrochemical oscillators. The electrooxidation of  $\text{C}_1$  organic molecules and the reduction of  $\text{Fe}(\text{CN})_6^{3-}$  are used for examples of the two categories of oscillators, respectively. According to the classification from the point of view of electrode processes,<sup>6</sup> the two categories of oscillators stem from the combination of electrochemical reactions (charge transfer) principally either with (i) surface steps (*e. g.* ad/desorption) or with (ii) mass transfer (*e. g.* diffusion, convection). The former example systems are subjects of many researches owing to their significance in energy conversion and reaction mechanisms. Nevertheless, systematic impedance spectra are still missing, and a definite connection between cyclic voltammogram and instability is also absent except for our

preliminary report.<sup>6</sup> Whereas the latter example oscillator is encountering a difficulty with two different explanations, in which convection feedback<sup>6-8</sup> and negative differential resistance (NDR)<sup>9</sup> are emphasized, respectively.

## Experimental

Electrochemical measurements were carried out with a CHI 660A Electrochemical Station (CH Instruments, Inc., USA) interfaced with a computer. A conventional H-type glass cell was used with three electrodes: a large strip of platinum, a platinum wire (1 mm in diameter and 8.5 mm in length) or a gold disk (2 mm in diameter) and a saturated calomel electrode (SCE) connected with a Luggin capillary, served as the counter, working and reference electrode, respectively. The working electrode was polished with emery paper and then was cleaned with ultrasonic waves, followed by electrochemical cleaning in the background solution of H<sub>2</sub>SO<sub>4</sub> (1 mol/L) until repeatable cyclic voltammograms were obtained. All solution was freshly prepared from doubly distilled water and analytical grade chemicals. Impedance spectra were measured at a potential control, and were expressed in Nyquist diagrams. *In situ* Raman spectra were obtained with a LabRam I confocal Raman spectrometer (Dilor, France)<sup>10</sup> on a roughened platinum disk (2 mm in diameter) with a roughness factor about 150. The exciting wavelength was 632.8 nm from an air-cooled He-Ne laser with a power of ca. 12 mW. The collection time for recording a single spectrum was 50 s.

## Results and discussion

### Oxidation of C<sub>1</sub> organic molecules on Pt

The cyclic voltammograms in Fig. 2a on the platinum wire electrode show that hydrogen ad/desorption and oxygen reduction are repressed in the presence of methanol. Only a very small oxygen reduction peak can be observed when the upper potential limit is set at 1.5 V where oxygen evolution occurs. While the upper potential limit is over 0.4 V, the oxidation current for the backward scan is larger than that for the forward scan in a range of potentials, and crossing cycles appear. When the potential is reversed in the ascending branch of the first oxidation peak, the backward curve is always above the

forward one until they intersect in the region of double layer. A second cross appears in the first ascending branch when the potential is reversed at 0.8 V in the first descending branch or at 1.5 V in the third ascending branch. These facts imply that a strong enough negative feedback step lies in the first ascending branch, which coincides with the upper potentials of the oscillation during the current scan (Fig. 2c). The negative feedback step might result from the removal of CO<sub>ad</sub> by the reaction with OH<sub>ad</sub> as suggested by the majority of literature. The *in situ* Raman spectra (Fig. 3) seem to support the suggestion. The band intensity for Pt—C vibration of the adsorbed carbon CO<sub>ad</sub> at about 490 cm<sup>-1</sup> decreases with potential increase. When the potential is beyond 0.4 V, the band disappears. It reappears at 0.3 V but has smaller band intensity when the potential is negative-going. This

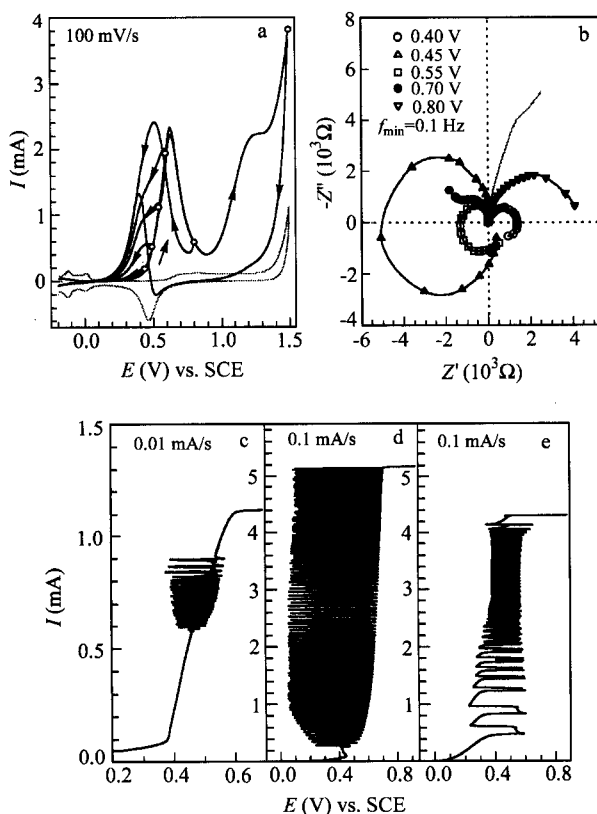


**Fig. 2** (a) Cyclic voltammograms and (b) Nyquist diagrams on a platinum wire electrode for the background solution of 1 mol/L H<sub>2</sub>SO<sub>4</sub> (the gray lines) and for 0.5 mol/L methanol solution (the black lines). Circles in (a) indicate different upper potential limits. The gray line in (b) is at 0.6 V. (c)–(e) Potential oscillations by current scan for 0.5 mol/L methanol, formaldehyde and formic acid, respectively.

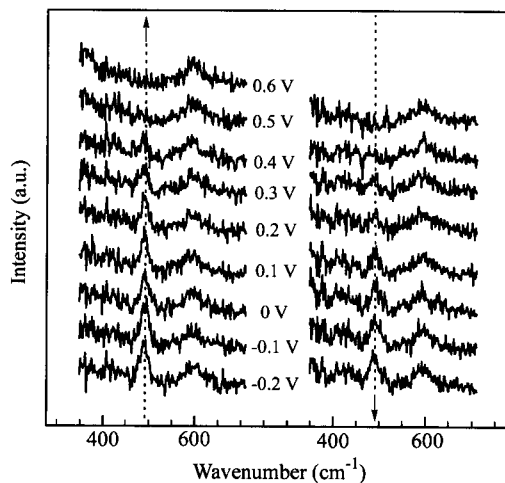


**Fig. 3** Raman spectra for 0.5 mol/L methanol solution on the roughened Pt disk with the potential increase and then decrease as indicated by the arrows. The vibrational band of  $490\text{ cm}^{-1}$  comes from the Pt—C of the linearly bound CO.

hysteretic phenomenon might account for the larger backward oxidation current in the cyclic voltammograms (Fig. 2a). In other words, the larger reverse scan current is due to the methanol oxidation on an un- and less poisoned surface. The electrode surface becomes poisoned again during the backward scan when the potential enters the hydrogen adsorption region accompanying an increase of the Pt—C vibration band intensity. It is the CO adsorption from methanol dissociation that depresses the hydrogen ad- and desorption, as well as the oxidation of methanol in the lower potential range during the forward scan. The formation and removal of  $\text{CO}_{\text{ad}}$  probably consist of the main positive and negative feedback steps in the crossing cycles (Fig. 2a) and the oscillations (Fig. 2c). The Nyquist plots for the oxidation of methanol (the lines with symbols) in Fig. 2b were obtained at different potential controls. With the increase of potential, the real part of the impedance ( $Z'$ ) for a range of higher frequencies varies from positive to negative, and then becomes positive again in the potential range 0.4, 0.45–0.7 V and  $\geq 0.8$  V, respectively. The negative  $Z'$  appears also in the first ascending branch where the initial backward scan current is always larger than the forward scan current (Fig. 2a). The formation of a (hydr)oxide layer has been attributed to be responsible for the negative  $Z'$  by Koper.<sup>5</sup> In addition, the  $Z'$  also varies with frequency, and a change from negative at a higher frequency to positive at a lower frequency (0.1 Hz) can be observed at

0.45 V and 0.55 V, which may be due to an additional unidentified process according to Koper.<sup>5</sup> However, no negative  $Z'$  could be measured in the background solution of  $\text{H}_2\text{SO}_4$  (1 mol/L) no matter what the potential is, and one of the plots is given in Fig. 2b (the gray line without symbol). Thus the methanol oxidation process, rather than the formation of (hydr)oxide layer only, is the main reason for the negative  $Z'$ .

Crossing cycles, negative  $Z'$ , and potential oscillations have also been observed for the electrooxidation of other  $\text{C}_1$  organic molecules. Only the potential oscillations are given here in Figs. 2d and 2e for formaldehyde and formic acid, respectively.

#### *Oxidation of $\text{C}_1$ organic molecules on Au*

Whereas on the gold electrode, only ordinary cyclic voltammograms appear (Fig. 4A), and there is no observable current for the oxidation of methanol. The oxidation peak current of formic acid is larger than that of formaldehyde but appears in a more positive potential. Unlike that on the platinum electrode, the reduction peak for the oxygen species on the gold electrode remains nearly unchanged in the presence of  $\text{C}_1$  organic molecules. It is naturally figured out from these facts that the adsorbed oxygen species are involved and uninvolved on the platinum and gold electrodes, respectively, in the electrocatalytic oxidation of  $\text{C}_1$  organic molecules.

Typical Nyquist plots for  $\text{C}_1$  organic molecules on the gold electrode are shown in Fig. 4B. Because the  $Z'$  is always positive, only one illustrative diagram is shown in Fig. 4B for each system: background (a), methanol (b), formaldehyde (c) and formic acid (d) solution.

Since there are no crossing cycles and no negative  $Z'$  in the oxidation of  $\text{C}_1$  organic molecules on the gold electrode, it is reasonable that no oscillations can be obtained during the current scan (Fig. 4C) according to the two criteria.

As a brief summary of the above results, both criteria are applicable to the oxidation of  $\text{C}_1$  organic molecules mainly involving surface steps.

#### *$\text{Fe}(\text{CN})_6^{3-}$ reduction with two different second current carriers<sup>11</sup>*

Further examination of the two criteria is extended to the category of oscillators mainly involving mass transfer.

There is a limiting current plateau in the reduction of  $\text{Fe}(\text{CN})_6^{3-}$ , and potential oscillations appear above the limiting current (the dashed lines of Figs. 5a and 5b, respectively). The oscillatory amplitudes are within the plateau region, and periodic hydrogen evolution was observed at the lower potential side of the plateau. When the solution also contains  $\text{IO}_3^-$ , the extra current over the limiting current is transferred by the reduction of  $\text{IO}_3^-$  instead of by the hydrogen evolution, and no oscillations occur in the same range of current scan (the solid lines of Figs. 5a and 5b, respectively).

The crossing cycle in the cyclic voltammograms of Fig. 5c (the dashed line) clearly shows the positive and negative feedback steps. They result from the depletion

(forward scan) and replenishment (backward scan) of the  $\text{Fe}(\text{CN})_6^{3-}$  surface concentration by diffusion-limited reduction and by convection-enhanced mass transfer from hydrogen evolution, respectively, and account for the potential oscillations between the bistability (with and without hydrogen evolution at the lower and upper potential sides of the limiting current plateau).<sup>7</sup> When the reaction in the second ascending branch is replaced by the reduction of  $\text{IO}_3^-$  (the solid line of Fig. 5c), the crossing cycle disappears in the absence of one feedback step from the convection mass transfer induced by the hydrogen evolution. That is the reason why there is no oscillation over the limiting current while both  $\text{Fe}(\text{CN})_6^{3-}$  and  $\text{IO}_3^-$  are present.

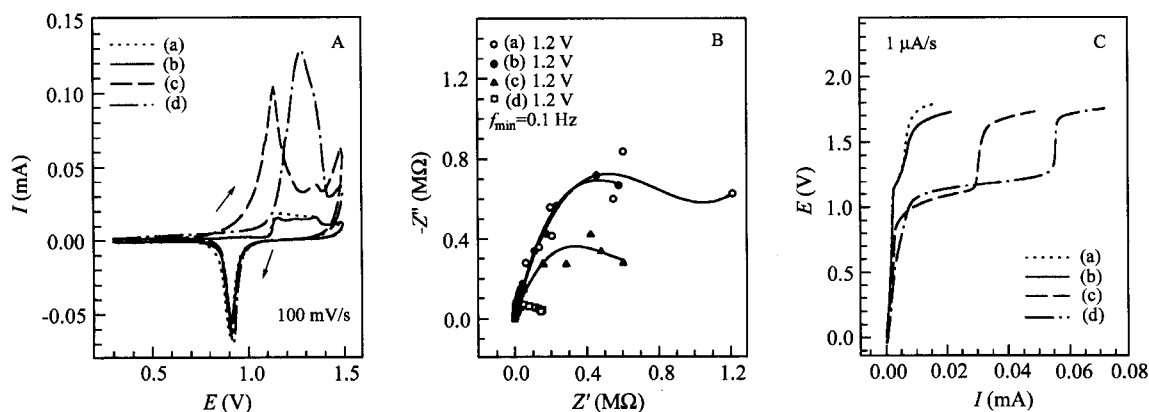


**Fig. 4** (A) Cyclic voltammograms, (B) Nyquist diagrams, and (C) potential-current curves (by current scan) on the gold disk electrode for solutions of (a)'s 1 mol/L  $\text{H}_2\text{SO}_4$ , plus 0.5 mol/L (b)'s methanol, (c)'s formaldehyde, and (d)'s formic acid.

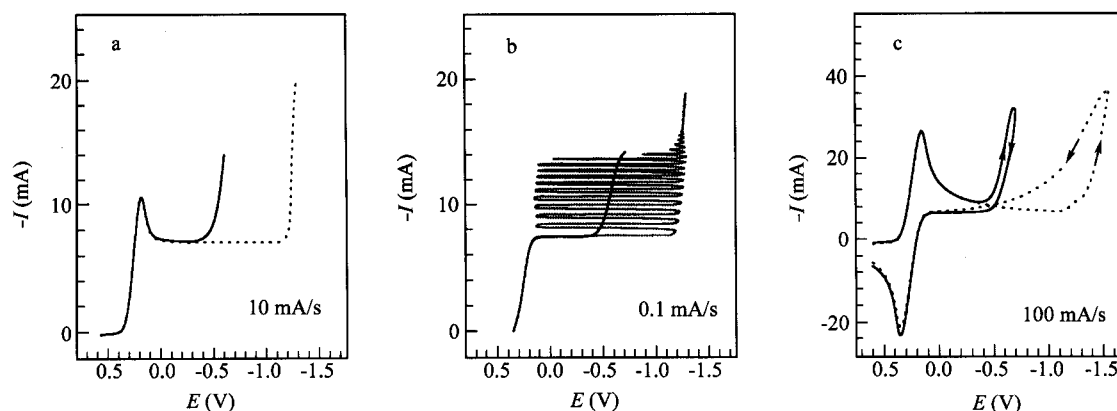


**Fig. 5** Potential-current curves by (a) potential scan or (b) current scan, (c) cyclic voltammograms for 0.6 mol/L  $\text{Fe}(\text{CN})_6^{3-}$  + 0.1 mol/L  $\text{IO}_3^-$  (the solid lines) or for 0.6 mol/L  $\text{Fe}(\text{CN})_6^{3-}$  (the dashed lines) on the platinum wire electrode with 1 mol/L NaOH as the supporting electrolyte.

However, negative  $Z'$  exists in the limiting current plateau for the systems of not only  $\text{Fe}(\text{CN})_6^{3-}$ ,<sup>7</sup> but also  $\text{IO}_3^-$ .<sup>9</sup> In other words, the a. c. impedance is insufficient to distinguish the two different situations as the cyclic voltammetry does since the convection mass transfer cannot be reflected in the impedance diagram. So the model<sup>9</sup> that emphasizes the negative differential resistance (NDR) stemming from the Frumkin repulsive effect without considering the induced convection feedback from hydrogen evolution is unacceptable.<sup>11-12</sup> Because the NDR is only responsible for the positive feedback step in this case, the impedance-based criterion is not applicable to this category of oscillators involving also the negative feedback step of convection mass transfer.

The voltammetry-based criterion not only has a wider range of applications, but also some other advantages. For example, it is more intuitive and less time-consuming than the a. c. impedance method. The overall profile in the interested potential range can be obtained from a single cyclic voltammogram, but the impedance measurement needs to select the potential one by one and takes a much longer time with a lower frequency limit.

## References

- 1 Fechner, M. G. T. *Schweigger J. für Chemie Physik* **1828**, 53, 129.
- 2 Wojtowicz, J. In *Modern Aspects of Electrochemistry*, Vol. 8, Eds.: Bockris, J. O' M.; Conway, B. E., Plenum Press, New York, **1972**, p. 47.
- 3 Hudson, J. L.; Tsotsis, T. T. *Chem. Eng. Sci.* **1994**, 49, 193.
- 4 Koper, M. T. M. In *Adv. Chem. Phys.*, Vol. 92, Eds.: Prigogine, I.; Rice, S. A., John Wiley & Sons, New York, **1996**, p. 161.
- 5 Koper, M. T. M. *J. Electroanal. Chem.* **1996**, 409, 175.
- 6 Li, Z. L.; Yu, Y.; Liao, H.; Yao, S. Z. *Chem. Lett.* **2000**, (4), 330.
- 7 Li, Z. L.; Cai, J. L.; Zhou, S. M. *J. Electroanal. Chem.* **1997**, 432, 111.
- 8 Li, Z. L.; Cai, J. L.; Zhou, S. M. *J. Electroanal. Chem.* **1997**, 436, 195.
- 9 Strasser, P.; Lübke, M.; Eickes, C.; Eiswirth, M. *J. Electroanal. Chem.* **1999**, 462, 19.
- 10 Tian, Z. Q.; Ren, B.; Mao, B. W. *J. Phys. Chem. B* **1997**, 101, 1338.
- 11 Li, Z. L.; Yuan, Q. H.; Ren, B.; Xiao, X. M.; Zeng, Y.; Tian, Z. Q. *Electrochem. Commun.* **2001**, 3, 654.
- 12 Li, Z. L.; Ren, B.; Xiao, X. M.; Zeng, Y.; Chu, X.; Tian, Z. Q. *J. Phys. Chem. B* **2002**, in press.

(E0106011 ZHAO, X. J.; DONG, H. Z.)